Exploring Intra-Annual Variations of Urban Effects on Precipitation in the Atlanta, GA, USA Region.

by

Olamiposi Fagunloye

Under the Direction of Jeremy E. Diem, Ph.D.

A Thesis Submitted in Partial Fulfillment of the Requirements for the Degree of

Master of Science

in the College of Arts and Sciences

Georgia State University

2024

ABSTRACT

Urban areas influence precipitation, but it remains unclear how these urban effects vary throughout the year. Therefore, this thesis examines monthly urban effects on precipitation variables in the Atlanta region. Precipitation totals, precipitation days, and heavy-precipitation days from 70 precipitation gauges over ten years (2014–2023) were analyzed. Key methods included spatially interpolating precipitation values, assessing correlations between precipitation and upwind imperviousness, and comparing precipitation at downwind gauges with control gauges. Urban effects on precipitation always occurred to downwind (i.e., east/northeast) of Atlanta). Precipitation totals and heavy-precipitation days were enhanced during May, July, and August. Precipitation totals and heavy-precipitation days were suppressed during February and March. Precipitation days were enhanced during most months. Likely mechanisms include the urban heat island effect (UHI) and urban aerosols, with the UHI causing the summer enhancement of precipitation and the aerosols causing both suppression and enhancement of precipitation.

INDEX WORDS: Urbanization, Precipitation, Urban heat island, Atlanta, Intra-annual variability, Enhancement, Suppression

Exploring Intra-Annual Variations of Urban Effects on Precipitation in the Atlanta, GA, USA Region.

by

Olamiposi Fagunloye

Committee Chair: Jeremy Diem

Committee: Jeremy Diem

Dajun Dai

Flávia D. S. Moraes

Electronic Version Approved:

Office of Graduate Services

College of Arts and Sciences

Georgia State University

December 2024

DEDICATION

First and foremost, I dedicate this work to God Almighty, whose grace and guidance have been my anchor throughout this journey. Without His divine wisdom and strength, none of this would have been possible. To my family, whose unwavering love, support, and encouragement have carried me through the challenges and triumphs of this research. To my parents, for nurturing my dreams and instilling in me the values of hard work and perseverance. To my friends, for their constant motivation and belief in me. Lastly, to my mentor, Dr. Jeremy Diem, for his invaluable guidance and support in shaping this research.

ACKNOWLEDGEMENTS

First, I thank God for His guidance and strength throughout this journey. I am deeply grateful to my advisor, Dr. Jeremy Diem, for his exceptional mentorship and support. My heartfelt thanks also go to my committee members, Dr. Flávia D. S. Moraes and Dr. Dajun Dai, for their invaluable feedback and guidance. I extend my appreciation to my family and friends for their unwavering support and encouragement. Lastly, I thank the Department of Geosciences at Georgia State University for providing the resources essential for this research.

TABLE OF CONTENTS

LIST OF FIGURES

LIST OF ABBREVIATIONS

UHI – Urban Heat Island

CSA – Combined Statistical Area

TRMM – Tropical Rainfall Measuring Mission

GPM – Global Precipitation Measurement

NOAA – National Oceanic and Atmospheric Administration

GHNd – Global Historical Climatology Network daily

NLCD – National Land Cover Database

HPD – Heavy Precipitation Days

PT – Precipitation Totals

PD – Precipitation Days

MM – Millimeter

NASA – National Aeronautics and Space Administration

GIS – Geographic Information Systems

PREFACE

This thesis is the culmination of my academic journey in the field of geosciences, exploring the dynamic relationship between urbanization and precipitation patterns in Atlanta, Georgia. It reflects my passion for understanding environmental changes and their impact on urban areas, shaped by my time at Georgia State University.

The research presented here was inspired by the growing need to address urban climate challenges, especially as cities expand and alter natural weather patterns. Throughout this process, I was fortunate to be guided by my advisor, Dr. Jeremy Diem, whose expertise and support have been crucial in shaping my work. The insights provided by my committee members, Dr. Flávia D. S. Moraes and Dr. Dajun Dai, were invaluable in refining my research.

This work required the use of multiple data sources and analytical methods, and I am grateful to have had access to the necessary resources and tools. The collaborative environment at Georgia State University and the encouragement from my peers and mentors helped bring this project to completion.

I hope this thesis contributes to the growing body of knowledge on urban climatology and serves as a stepping stone for future research in this field.

1 INTRODUCTION

Urbanization, a pervasive global process, dramatically reshapes the environment and triggers a cascade of environmental challenges. In recent decades, urban land has expanded globally at approximately 5% per decade (Güneralp et al., 2020). This expansion is linked to the fragmentation of natural habitats (Liu et al., 2016; Li et al., 2022), leading to significant disruptions in ecosystems and a decline in biodiversity (Simkin et al., 2022; Kondratyeva et al., 2020). Urbanization has also been identified as a factor that exacerbates extreme precipitation events (Mukherjee et al., 2018). The urban heat island (UHI) phenomenon, characterized by elevated air temperatures in urban areas due to the replacement of vegetation with heat-absorbing surfaces, is a direct consequence of urbanization (Bornstein, 1968; Oke, 1973; Draxler, 1986; Oke, 1987). Urban areas have been the primary source of greenhouse gas emissions, with CO_2 being the main contributor to the total rise in greenhouse gas emissions (Luqman et al., 2023). Furthermore, urban areas are known for their high concentrations of air pollutants (Feng et al., 2017), primarily from industrial activities, and energy production, which pose significant risks to environmental health and contribute to illness and premature death (Liang & Gong, 2020).

Among the various impacts of urbanization, precipitation modification is important because of its impact on water resources. The implications of these changes are far-reaching and potentially devastating (Deng et al., 2023). For instance, the expansion of impervious surfaces in urban areas has been linked to increased surface runoff and a heightened risk of flooding, a pressing concern for urban planners and residents alike (Lu et al., 2023). This is particularly concerning given the increasing trend of urbanization globally (Zhang, 2016). In Shanghai, China, urbanization has not only altered the characteristics of extreme precipitation but also increased its variability (Mou et al., 2022). Similarly, in Beijing, China, urbanization has been found to reduce rainfall in urban areas while increasing it downwind of the city (Liu et al., 2021). Furthermore, pollutants from urban and industrial sources have been found to disrupt the natural processes within clouds that lead to precipitation, effectively dampening the formation of rain and snow by preventing water droplets from merging (Rosenfeld, 2000).

Urbanization influences precipitation through various processes. Impervious surfaces, such as asphalt, can cause urban areas to be about 3° C warmer than they would be otherwise (Estoque et al., 2017; Yang et al., 2022; Wang et al., 2022). These increased temperatures, which create the UHI effect, can intensify atmospheric instability and stimulate and enhance convective precipitation (Arnfield, 2003; Dixon & Mote, 2003). Landscape changes from urbanization increase surface roughness (Chang et al., 2021; Hou et al., 2023; Rajeswari et al., 2021). The increased roughness can disrupt wind flow and influence the development and movement of convective systems (Gunawardena et al., 2017; Chang et al., 2021). Additionally, urban areas typically have a disproportionate number of small aerosols due to excessive fossil-fuel combustion (Çiçek & Turkoglu, 2005; Le et al., 2019; Huang et al., 2023). This can suppress rainfall by producing a narrow droplet spectrum that inhibits collision and coalescence processes in clouds, thereby slowing down the formation of larger, rain-producing droplets (Tao et al., 2012; Singh et al., 2020).

Various types of data have been used to study the impact of urbanization on precipitation. Gauge-based precipitation data from meteorological gauges have been widely used to analyze rainfall patterns and trends in urban and rural areas (Huff & Changning, 1972; Çiçek & Turkoglu, 2005; Diem & Mote, 2005; Daniels et al., 2015). In addition, satellite-based rainfall estimates, such as those from the Tropical Rainfall Measuring Mission (TRMM) and Global Precipitation Measurement (GPM), have been used to examine urban effects on precipitation at larger spatial scales (Shepherd et al., 2002; Ali et al., 2021). Nevertheless, the level of detail in products like TRMM might not be sufficient to effectively identify the impact of urban areas on rainfall (Diem et al., 2004). Ground-based radar data have also been employed to investigate precipitation's spatial distribution and intensity in urban areas (Mote et al., 2007). Some studies (Deng et al., 2023; Chang et al., 2021) have combined multiple data sources, such as gauge, satellite, and radar data, to provide a comprehensive assessment of urban impacts on precipitation.

Previous research has generally found that urbanization increases rainfall in the summer. Many studies show urbanization leading to increased precipitation and downwind in urban areas (Huff & Changnon, 1972; Shepherd et al., 2002; Diem & Brown, 2003; Mote et al., 2007; Diem, 2008; Georgescu et al., 2012; Daniels et al., 2015; McLeod et al., 2017; Deng et al., 2023). Some examples of these are as follows: a 10–20% increase in precipitation downwind of St. Louis (Huff & Changnon, 1972); daily precipitation totals downwind of urban areas were about 7% higher than precipitation in the rest of the Dutch West Coast (Daniels et al., 2015); approximately 28% increase within a 30–60 km radius downwind of Atlanta, Georgia; Montgomery, Alabama; Nashville, Tennessee; and San Antonio, Waco, and Dallas, Texas (Shepherd et al., 2002). Urbanization can also increase the frequency of heavy precipitation days or rainfall extremes (Çiçek & Turkoglu, 2005; Mukherjee et al., 2018; Zhang et al., 2018; Fagnant et al., 2020; Singh et al., 2020; Ali et al., 2021; Yu et al., 2022). Some examples of this are as follows: a 50% increase in the number of heavy precipitation days at an urban station in Ankara compared to a rural station (Çiçek & Turkoglu 2005), rainfall extremes substantially increasing the probability of a 25% change in 50-year events in urban areas by 2.7 times compared to rural areas in the United States (Singh et al., 2020), and a 26.4% increase in heavy precipitation in the Yangtze River Delta (YRD) urban areas of East China (Yu et al., 2022).

In the existing body of research, there are notable gaps that this study aims to address. A substantial number of studies (Singh et al., 2020; Liu et al., 2021; Diem & Brown, 2003; Mote et al., 2007; Diem and Mote, 2005; Miao et al., 2011; Diem, 2008; McLeod et al., 2017; Jo et al., 2020; Ashley et al., 2012; Bentley et al., 2012; Bornstein & Lin, 2000) focus primarily on the summer season, leaving other seasons relatively unexplored in the context of urbanization's impact on precipitation. Furthermore, most of these studies (Shepherd et al., 2002; Dixon & Mote, 2003; Debbage & Shepherd, 2015; Yilmaz & Perera, 2015; Mote et al., 2007; Islam et al., 2023) rely on data spanning approximately five years, which may be too short a period to adequately detect urban effects on precipitation. Some studies (Wang et al., 2010; Guhathakurta et al., 2011; Miao et al., 2011; Daniels et al., 2015) only examine precipitation totals and do not analyze other variables such as precipitation intensity and frequency. Finally, only several studies (Jauregui and Romales, 1996; Diem, 2008; Islam et al., 2023; Lu et al., 2023) have used at least 30 gauges in their analysis, which is important for ensuring robust spatial coverage and capturing regional variations in precipitation patterns. A higher number of gauges reduces the risk of spatial biases and improves the accuracy of detecting urbanization effects on precipitation across diverse landscapes (Daly et. al., 1994).

The purpose of this research is to investigate the impact of urbanization on precipitation throughout the year, using a comprehensive dataset spanning over ten years and incorporating data from a larger number of gauges. The objectives are as follows: (1) to determine the spatial variability of urban effects on precipitation; (2) to assess monthly differences in urban effects.

2 STUDY REGION

The chosen study region is centered on the Atlanta–Sandy Springs–Gainesville combined statistical area (CSA) in the southeastern United States (Figure 2.1). CSA serves as a model for studying the environmental and urbanization challenges faced by rapidly growing metropolitan regions worldwide (Kundell & Myszewski, 2002). As the largest metropolitan area in the Southeastern United States, its rapid population growth, which increased by over 24% between 2000 and 2010, exemplifies the pressures of urban sprawl on infrastructure, air quality, and water resources (Kundell & Myszewski, 2002). There are minimal effects on precipitation by topography and water bodies on precipitation in the region (Diem, 2008), as the long-term rainfall observation sites in the Atlanta metropolitan area are neither located near large bodies of water nor in regions with large elevation changes. The CSA has experienced significant growth over the last two decades; the population has grown from 4.9 million in 2000 to about 7.0 million in 2022 (Urban Areas Facts, 2021), leading to increased urbanization and impervious surfaces, which are critical factors in urban-induced precipitation changes. Seasonal precipitation in the region is largely driven by frontal systems during the winter and convective processes during the summer, which influences the accuracy of precipitation maps; errors are lower during the winter when precipitation is more spatially uniform (Diem, 2008). The region's rapid development and its representativeness of many growing metropolitan areas make it an ideal case study for examining the effects of urbanization on precipitation dynamics.

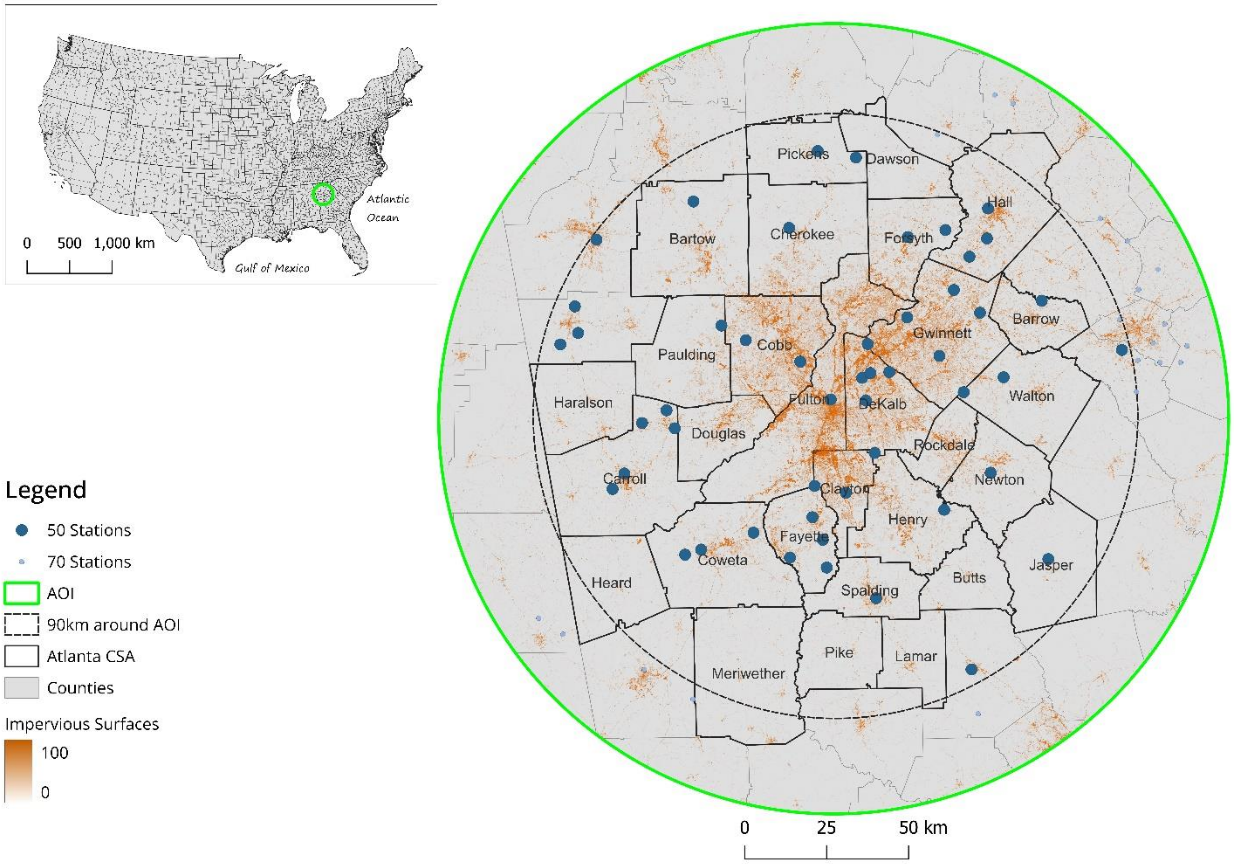

Figure 2.1 Map of the study region showing locations of the 70 precipitation gauges within 110 km of downtown Atlanta, the 50 precipitation gauges within 90 km of downtown Atlanta, the counties within the Atlanta–Sandy Springs–Gainesville combined statistical area (CSA), and imperviousness (%) throughout the domain. The inset map shows the Atlanta region within the southeastern United States.

3 DATA

3.1 Daily Precipitation

Daily precipitation totals during 2014-2023 for 70 gauges were obtained from the Global Historical Climatology Network daily (GHNd) database of the National Oceanic and Atmospheric Administration (NOAA). All gauges were within 110 km of downtown Atlanta and were missing no more than 15% of daily totals over the ten years. If two gauges were within 3 km of each other, only one station was retained to minimize spatial redundancy and ensure an even spatial distribution of observations, which is critical for reducing biases in regional precipitation analyses (Daly et al., 2008). The retained gauge was selected based on data completeness, reliability, local representativeness, and its contribution to a balanced spatial network. For the entire 70-station database, only 6.2% of station days were missing precipitation totals. If a station had a precipitation observation that occurred in the morning, the precipitation total was shifted to the previous day. Missing daily totals for a station were replaced by the mean total from the three nearest gauges.

3.2 Lower-Troposphere Winds

Daily U and V components of 700-hPa wind over the Atlanta region during 2014-2023 were obtained from NOAA's North American Regional Reanalysis (Shepherd et al., 2002). These data, with a 32-km spatial resolution, were selected because the 700-hPa level is commonly used to analyze low-level atmospheric flow, which is critical for understanding moisture transport and the movement of urban-induced convection (Diem, 2008; Shepherd, 2005). The U and V values for the Atlanta region were averaged across 26 grid cells to represent the mean wind flow over the study area. This analysis helps identify prevailing wind directions and their role in transporting aerosols and heat downwind, influencing precipitation patterns. The 700-hPa level is particularly relevant as it reflects mid-tropospheric dynamics, which are less influenced by surface friction and more representative of synoptic-scale flow impacting urban areas (Changnon, 1979). Previous urban-effects studies (Rose et al., 2008; Haberlie et al., 2014) in Atlanta also have used 700-hPa as the steering flow.

3.3 Impervious Surfaces

Gridded developed-imperviousness data were acquired for 2019 from the National Land Cover Database of the Multi-Resolution Land Characteristics Consortium. The dataset had a spatial resolution of 30 m. For each grid cell, the percentage of developed surface that was impervious was provided. This dataset is relevant as it enables the quantification of urbanization patterns, which are critical for understanding how urban land use influences precipitation patterns through phenomena such as the urban heat island effect.

4 METHODS

4.1 Analysis of 700-hPa Winds

The analysis of 700-hPa winds is essential for understanding how urbanized areas influence precipitation, as this level reflects the transport of heat, moisture, and aerosols that drive urban-induced precipitation patterns (Shepherd, 2005; Diem, 2008). To achieve this, histograms of wind directions for each month were generated, providing a visual representation of air flow throughout the year. In addition, month-specific box-and-whisker plots of daily precipitation totals, precipitation days, and heavy precipitation days for each of eight wind directions (i.e., North, Northeast, East, Southeast, South, Southwest, West, and Southwest) were developed. A precipitation day has at least 1 mm of precipitation, while a heavy-precipitation day has at least 25 mm of precipitation. Precipitation data for the wind analyses were from the 50 gauges within 90 km of downtown Atlanta, selected to ensure accurate wind direction analysis by minimizing the edge/border effect that can occur with gauges near the study area's boundary.

4.2 Calculation of Upwind Urban Land

The calculation of upwind urban land is important in determining the influence of urban areas on precipitation. Upwind urban land refers to the urbanized area located in the direction from which the prevailing winds originate, while downwind urban land refers to urbanized areas located in the direction toward which the winds are blowing (Rath et al., 2021). Since urban effects on precipitation tend to exist for up to 80 km downwind of urban land (Mote et al., 2007), mean developed imperviousness within 20 km, 30 km, 40 km, 50 km, 60 km, 70 km, and 80 km of each NLCD grid cell was calculated. Calculations were performed for all eight wind directions using the Focal Statistics tool in ArcGIS Pro and a 45° wedge that extended from 20 to 80 km from each grid cell.

Surfaces representing upwind imperviousness for each month were created, using a method that integrates a weighted combination of eight distinct upwind urban land surfaces. Each of the eight wind directions were assigned a weight. These weights were determined by averaging the weights that were calculated based on various factors, including total precipitation, the number of days with precipitation, and the number of days experiencing heavy precipitation.

4.3 Spatial Analysis of Precipitation

For each month, surfaces of total precipitation, precipitation days, and heavy-precipitation days were generated to investigate the potential enhancement of precipitation downwind of urban areas, considering both all days in a month and days with the prevailing wind direction for that month. Total precipitation refers to the cumulative amount of rainfall in millimeters, while precipitation days represent the number of days with at least 1 mm of rainfall, and heavy-precipitation days are defined as days with at least 25 mm of rainfall. These variables capture different aspects of precipitation intensity and frequency, allowing for a more comprehensive understanding of urban impacts on precipitation patterns (Diem & Mote, 2005; Shepherd, 2005). Prevailing wind direction isolates the influence of urban aerosols and the urban heat island (UHI) under dominant synoptic conditions, which are key to understanding directional enhancements (Dixon & Mote, 2003). Data from all 70 gauges were used to ensure adequate spatial coverage and smoother interpolation results across the region (Daly et al., 2008).

Kriging, a geostatistical technique available in ArcGIS Pro (Xiao et al., 2016) will be used to generate surfaces. The accuracy of all surfaces will be assessed using cross-validation in

ArcGIS Pro, using percent error (i.e., root mean squared error divided by mean observed value) as the evaluation statistic. Ordinary Kriging was chosen for its suitability in modeling spatial autocorrelation under the assumption of a constant but unknown mean. The process involved fitting a semivariogram to the data, optimizing parameters (e.g., search radius and resolution), and validating the results through cross-validation to ensure reliable surface predictions.

4.4 Assessment of Correlations between Upwind Imperviousness and Precipitation

For each month, correlations between precipitation and upwind urbanization were calculated using Pearson product–moment correlation tests ($\alpha = 0.01$; one-tailed). Precipitation totals, precipitation days, and heavy precipitation days at the 50 gauges within 90 km of downtown Atlanta will be used. The urbanization variables will be the mean developed imperviousness and the amount of medium- and high-intensity developed land upwind of the 50 gauges, as these metrics are directly linked to urban-induced changes in precipitation through mechanisms such as increased runoff, altered evapotranspiration, and enhanced aerosol production (Shepherd, 2005; Diem, 2008). Medium- and high-intensity developed land are particularly relevant because they represent areas with dense impervious surfaces, which are closely associated with urban heat island effects and precipitation anomalies (Oke, 1987). Correlations also were calculated using residuals from regression models, a method commonly employed to isolate the effects of specific variables (e.g., urbanization) by accounting for confounding factors such as elevation (Daly et al., 2008; Diem, 2008). The residuals were essentially precipitation values with the effect of elevation removed, where elevation was the predictor and precipitation was the predictand in the models.

4.5 Precipitation at Downwind Gauges vs. Precipitation at Control Gauges

Differences in precipitation values between upwind and control gauges were analyzed for each month and imperviousness (e.g., 20-km upwind imperviousness) combination. The 32 gauges within 60 km of downtown Atlanta were used and, for each scenario, the ten gauges with least upwind imperviousness were classified as upwind gauges and the ten gauges with the most upwind imperviousness were classified as downwind gauges. A distance of 60 km from downtown Atlanta was used in order to minimize the effects of topographic differences among the gauges. Monthly precipitation totals, precipitation days, and heavy precipitation days were compared between the two groups using Mann-Whitney U tests ($\alpha = 0.01$, one-tailed).

5 RESULTS

5.1 Month-specific lower-troposphere flow and precipitation-associated wind directions

Lower-troposphere winds over the region were mostly westerly in general throughout the year with less westerly flow during May and October (Figure 5.1). During November-March, winds were predominantly westerly and southwesterly; a majority of the days in December, January, and February had westerly flow. There was a reduced westerly flow in April, May, and June, and the wind direction became even more balanced, with the westerly, northwest, and westerly flow occurring on between 30% and 40% of days. Flow from the north, east, and south became more prevalent during May-October. This increased balance of wind directions is epitomized in September.

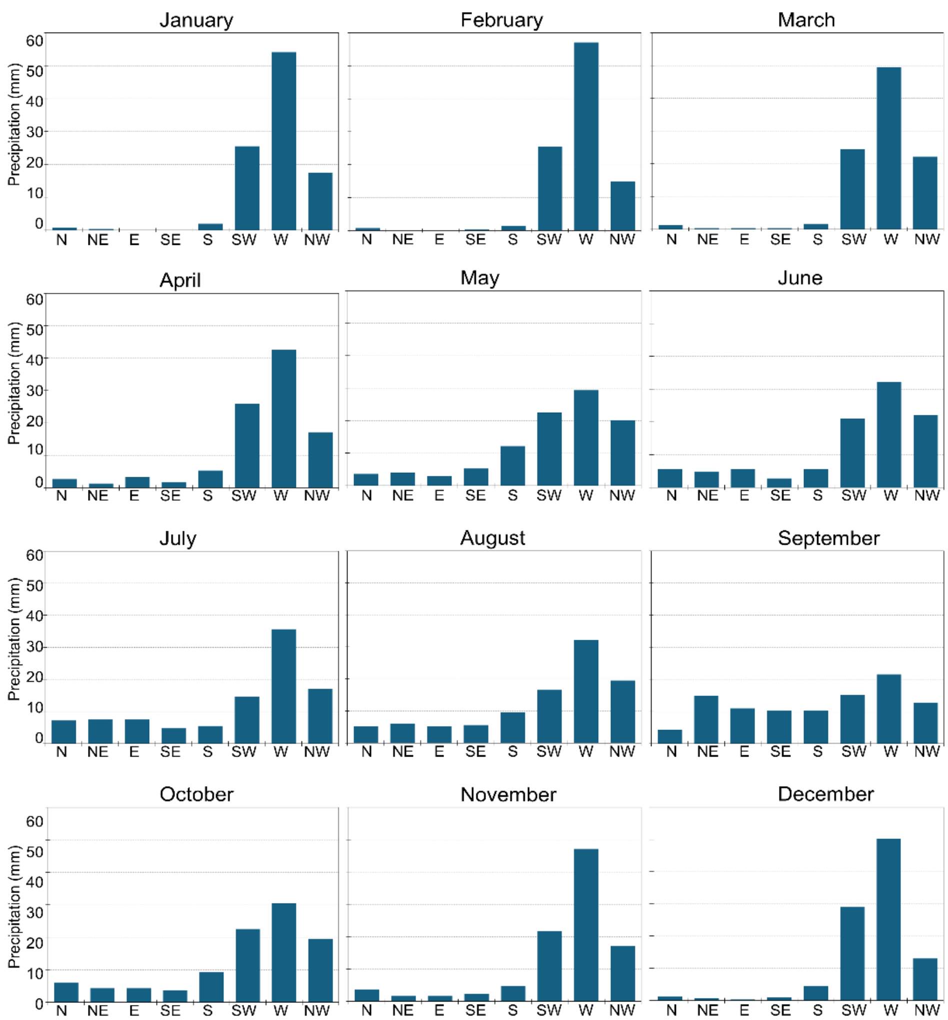

Figure 5.1 Month-specific frequency distributions of 700-hPa wind direction within the Atlanta-Sandy Springs-Gainesville CSA.

Precipitation was primarily associated with westerly and southwesterly flow for most months (Figures 5.2 – 5.4). Total precipitation for each month and wind direction shows substantial variability, with the highest totals generally occurring in the westerly and southwesterly wind directions across most months, especially during November-April. Similar to precipitation totals, precipitation days and heavy-precipitation days tended to be associated with southwesterly and westerly flow during most months, particularly noticeable in the winter and early spring months. Heavy-precipitation days, primarily during November-April, also tended to occur during westerly and southwesterly flow. During May-October, precipitation totals, precipitation days, and heavy-precipitation days were less restricted to westerly and southwesterly flow, and, as noted previously, September was the month with the most balance among the wind directions.

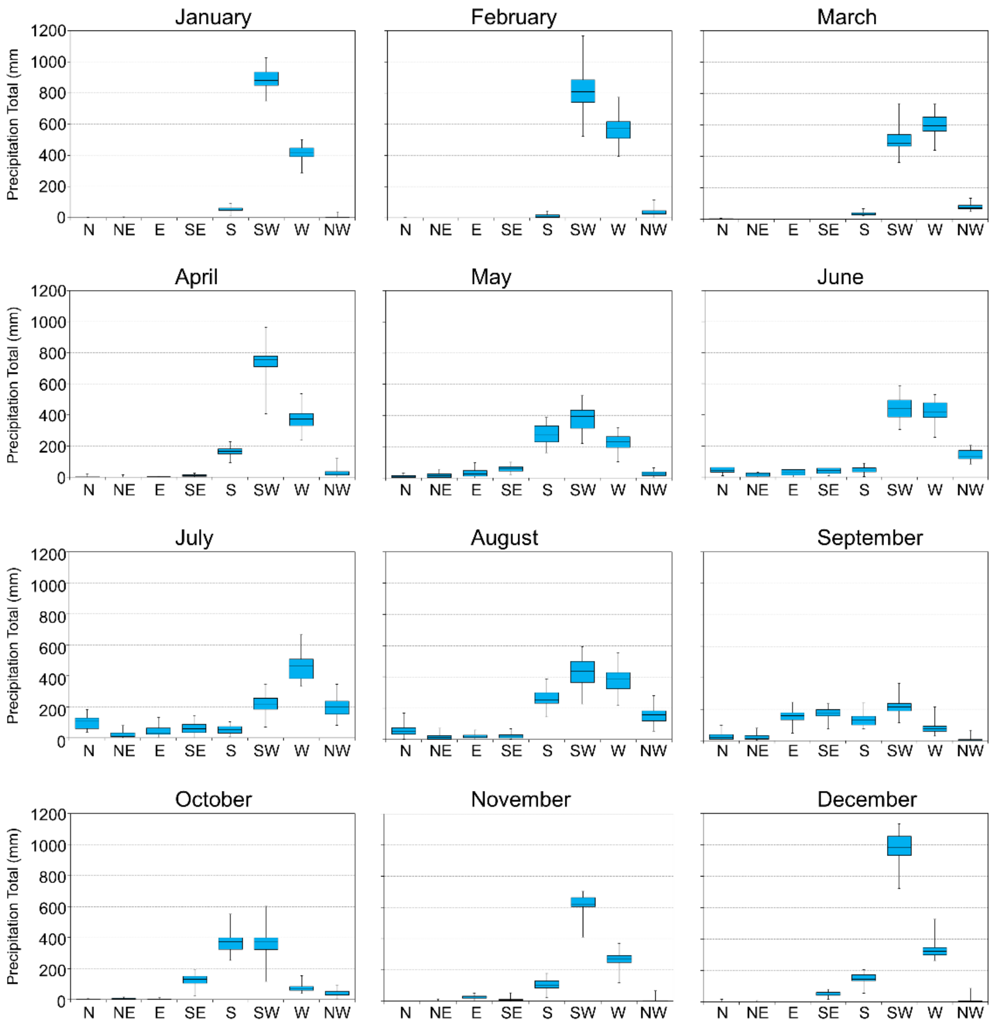

Figure 5.2 Month-specific box and whisker plots of precipitation totals for 700-hPa wind directions within the Atlanta-Sandy Springs-Gainesville CSA.

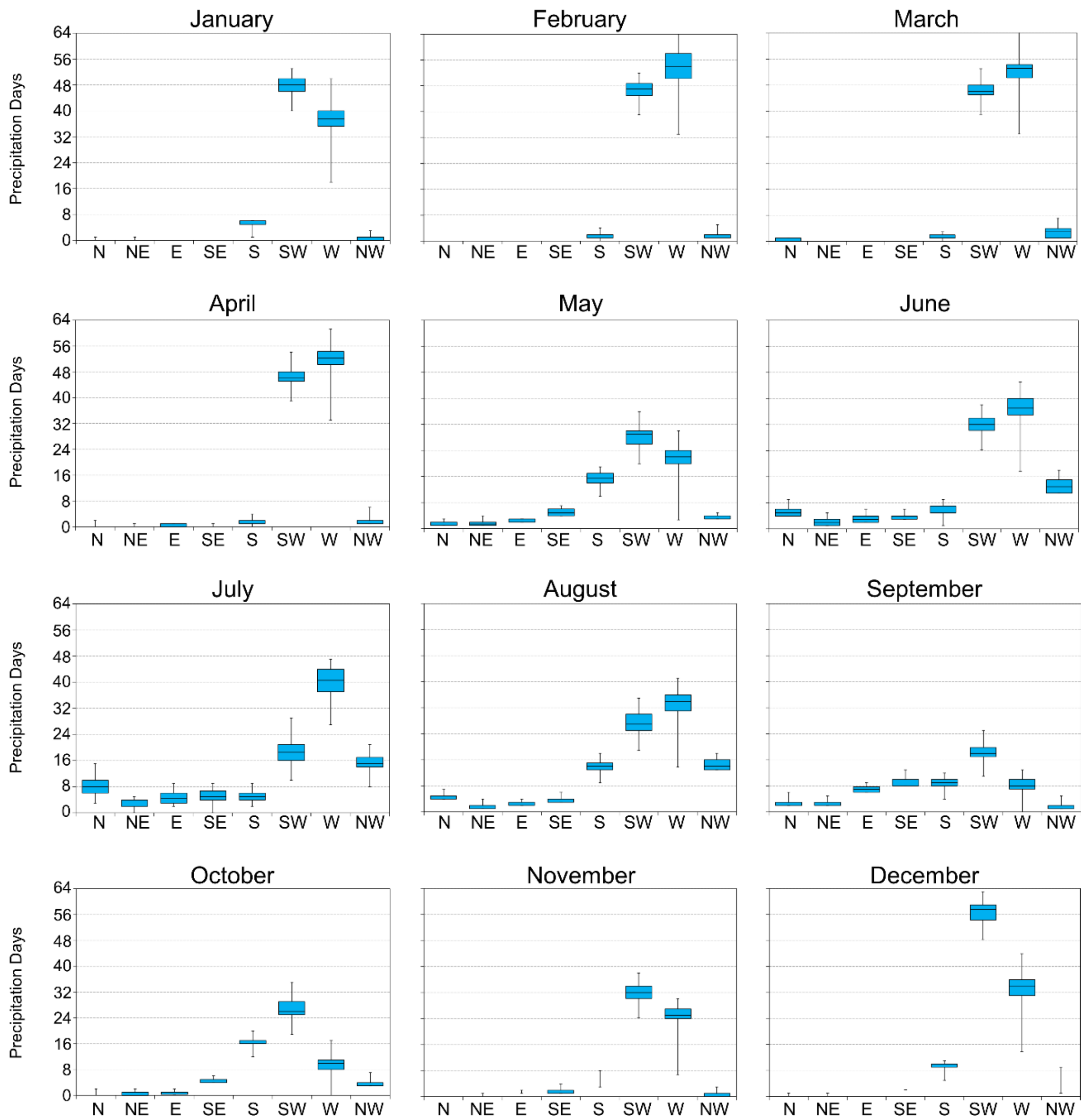

Figure 5.3 Month-specific box and whisker plots of precipitation days for 700-hPa wind directions within the Atlanta-Sandy Springs-Gainesville CSA.

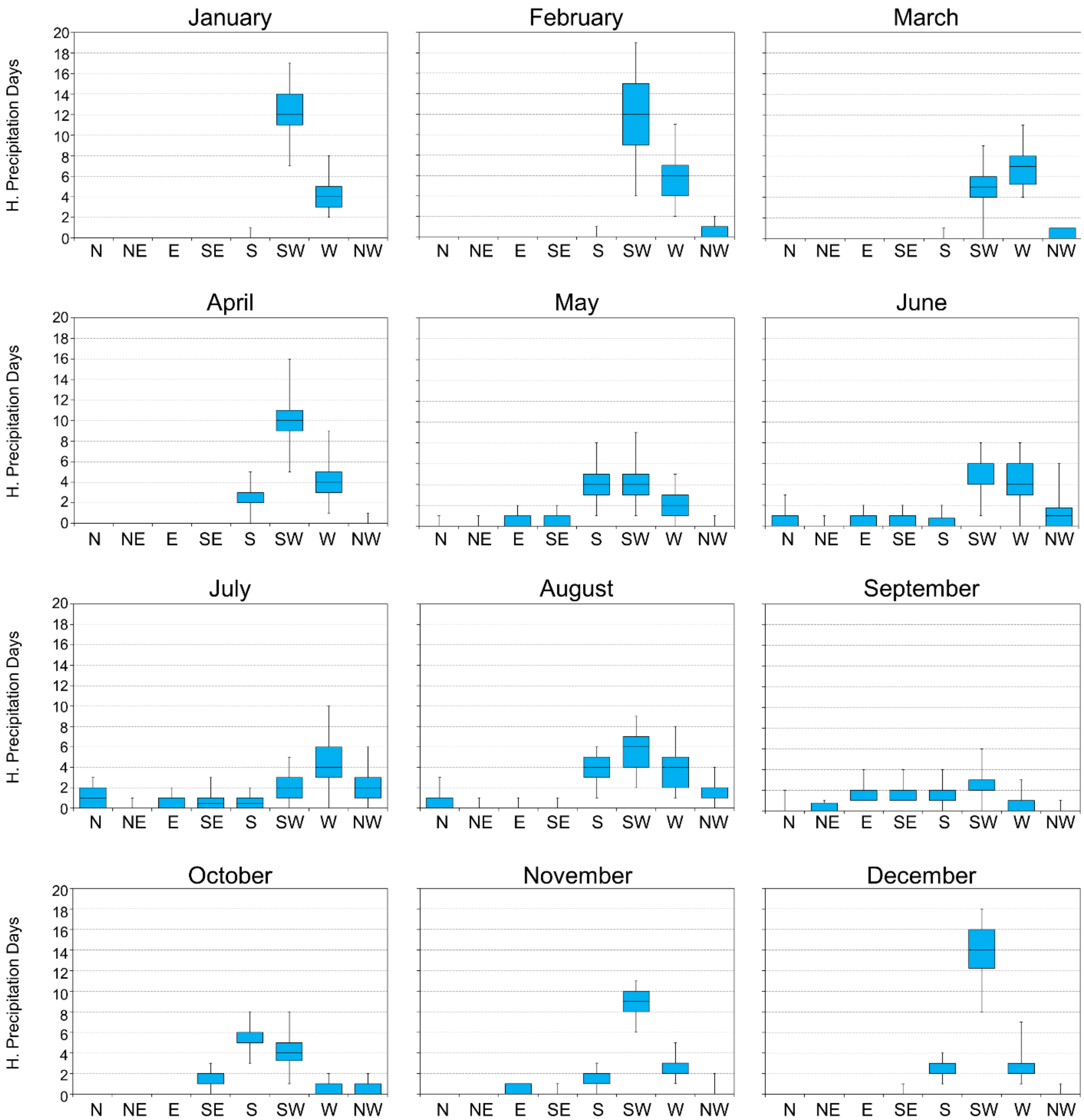

Figure 5.4 Month-specific box and whisker plots of heavy-precipitation days for 700-hPa wind directions within the Atlanta-Sandy Springs-Gainesville CSA.

5.2 Month-specific surfaces of mean imperviousness of 20 km, 50 km, and 80 km upwind associated with rainfall

Based on the mean imperviousness upwind of locations, urban precipitation enhancement appears most likely to occur over and to the east/northeast of Atlanta during nearly all months (Figure 5.5). The mean imperviousness 20 km upwind of locations is highest over and to the north/northeast of Atlanta, particularly in northern Fulton County, western DeKalb County, western Gwinnett County, and eastern Cobb County, with the maximum values occurring over western DeKalb County. As the upwind distance increases to 50 km, the mean imperviousness is greatest east and northeast of Atlanta, including DeKalb County, Gwinnett County, Rockdale County, Forsyth County, northern Fulton County, southern Hall County, and eastern Barrow County, with maximum values in Gwinnett County. The pattern differs in September and October, when the largest values are centered over northern Fulton County rather than Gwinnett County. At a distance of 80 km, mean imperviousness is highest in the northeastern portion of the region, including Gwinnett County, eastern Forsyth County, southern Hall County, eastern Jackson County, and eastern Barrow County, with maximum values over Gwinnett County and Hall County. During September and October, the maximum values shift northwestward to Forsyth County.

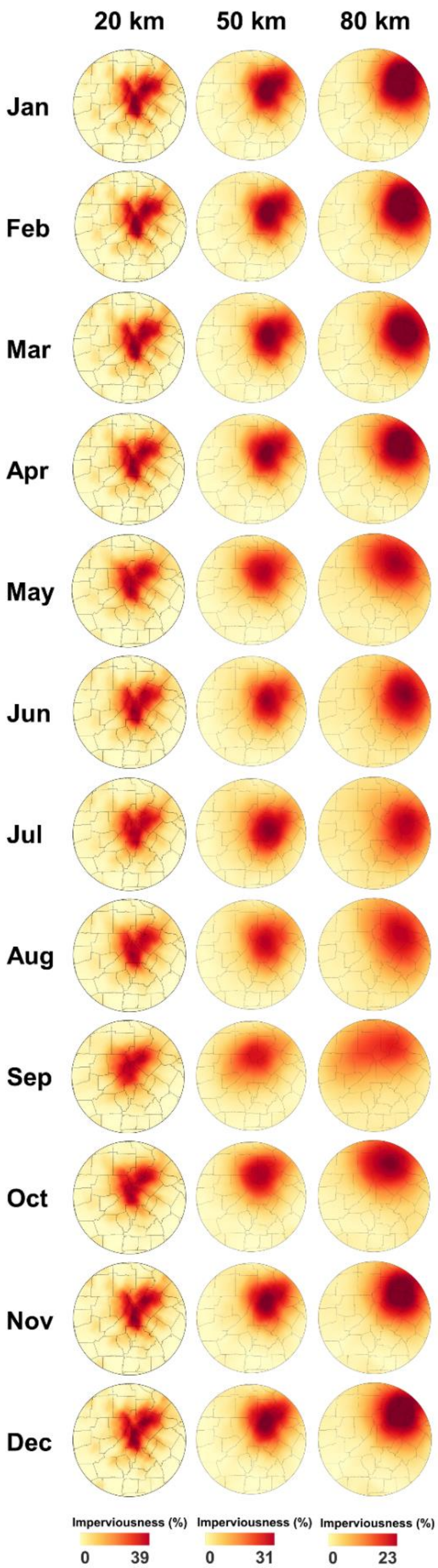

Figure 5.5 Percent imperviousness at 20 km, 50 km, and 80 km distances upwind of pixels for each month.

5.3 Month-Specific Cumulative Precipitation Frequency Surfaces

The spatial patterns of precipitation totals varied considerably among the months, with only July and August exhibiting the expected patterns related to urban-precipitation enhancement (Figure 5.6). In January, maximum precipitation occurred far to the southwest of Atlanta in Heard County. During February-April, maximum precipitation was recorded far to the north of Atlanta in Dawson County, with February and March showing more precipitation in the western portion of the study region compared to the eastern portion. In May, maximum precipitation occurred to the northeast of Atlanta in Hall and Jackson Counties. Maximum precipitation totals in June were located to the southwest of Atlanta in Fulton, Coweta, Heard, and Troup Counties. July and August had maximum precipitation totals over and slightly to the northeast of Atlanta in DeKalb and Gwinnett Counties. In September, maximum precipitation totals were found far to the northeast of Atlanta in Hall and Forsyth Counties. Finally, the maximum precipitation totals during October-December occurred far to the north/northeast of Atlanta in Dawson and Lumpkin Counties.

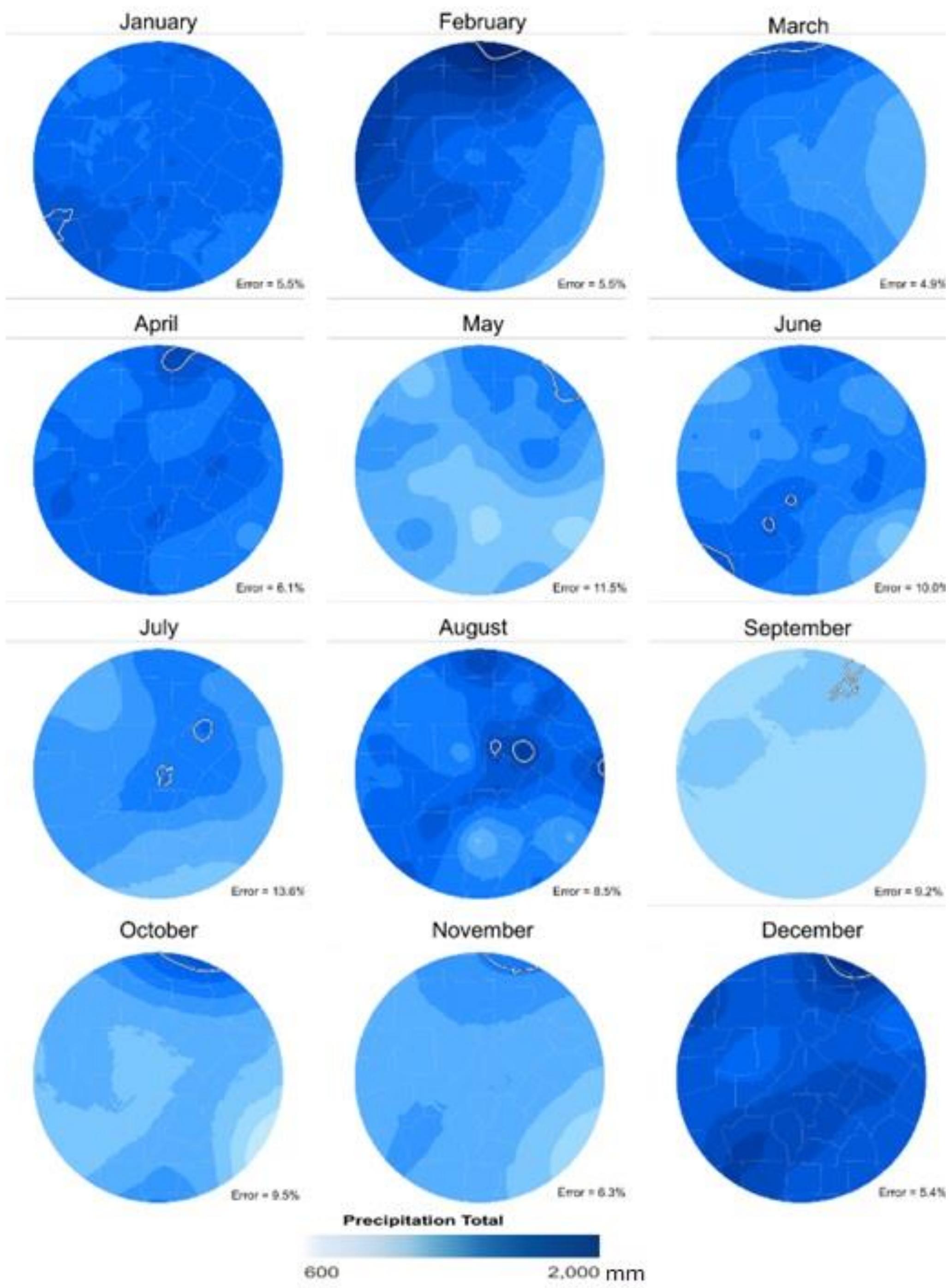

Figure 5.6 Month-specific surfaces of cumulative precipitation totals (mm) for the Atlanta region over 2014-2013 with the cross-validated percent error on each surface. White contour lines outline areas within the top 1% of precipitation totals.

The monthly maps of precipitation days showed greater consistency compared to the maps for precipitation totals, and the urban precipitation enhancement was less pronounced (Figure 5.7). The maximum number of precipitation days over the region occurs mostly in the far northern part of Atlanta, particularly in Pickens and Dawson Counties, across all months. September and November were the only months where a relatively high number of precipitation days occurred over and immediately downwind of Atlanta, specifically in DeKalb and Gwinnett Counties.

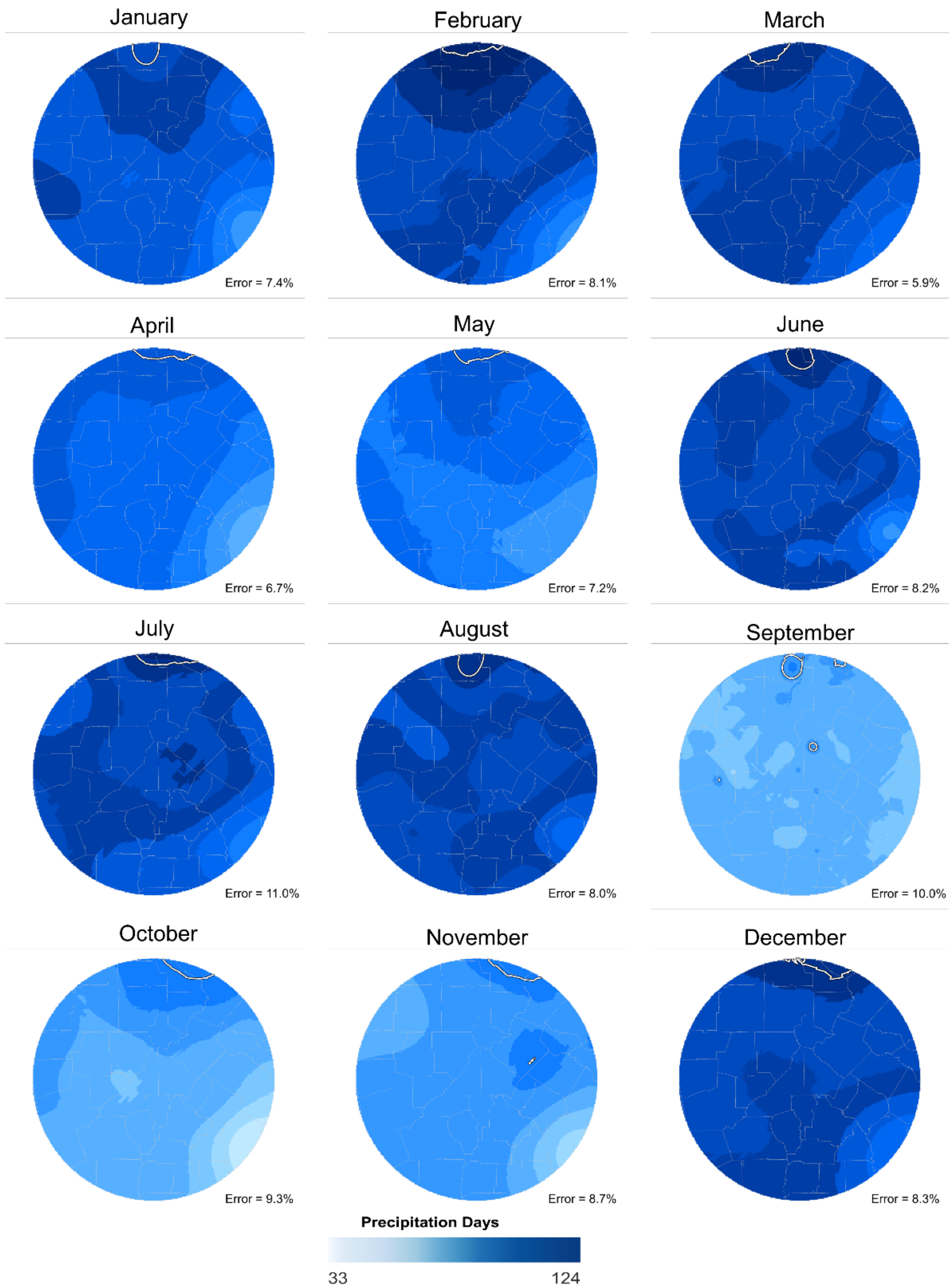

Figure 5.7 Month-specific surfaces of cumulative frequencies of precipitation days for the Atlanta region over 2014-2013 with the cross-validated percent error on each surface. White contour lines outline areas with the top 1% of values.

The variability in the number of heavy-precipitation days followed unique monthly patterns compared to precipitation days, and there is evidence of urban enhancement of precipitation during July, August, September, and December (Figure 5.8). The maximum number of heavy-precipitation days peaked downwind of Atlanta in Gwinnett, Forsyth, DeKalb, and Walton counties. In January and March, the maximum numbers of heavy-precipitation days occurred far to the west and southwest of Atlanta, specifically in Heard, Haralson, and Carroll Counties, while in February, the maximum values were far to the northwest of Atlanta. April, May, October, and November saw maximum values occurring far to the north/northeast of Atlanta, particularly in Dawson, Lumpkin, and Pickens Counties. Notably, November also had maximum values to the southwest of Atlanta in Troup, Meriwether, and Spalding Counties. June exhibited maximum values both far to the east and far to the southwest of Atlanta, in Heard and Jackson Counties, respectively. July's maximum values were scattered throughout the region, with some zones of maximum values over and immediately to the east of Atlanta in Gwinnett, Walton, and DeKalb Counties. Similarly, in August, maximum values occurred over and immediately to the east of Atlanta in DeKalb, Gwinnett, and Hall Counties. In September, maximum values were observed immediately to the northeast of Atlanta in Forsyth, Gwinnett, and Hall Counties. Finally, December had maximum values occurring immediately northeast of Atlanta in Gwinnett County and far to the southeast of Atlanta in Jasper County.

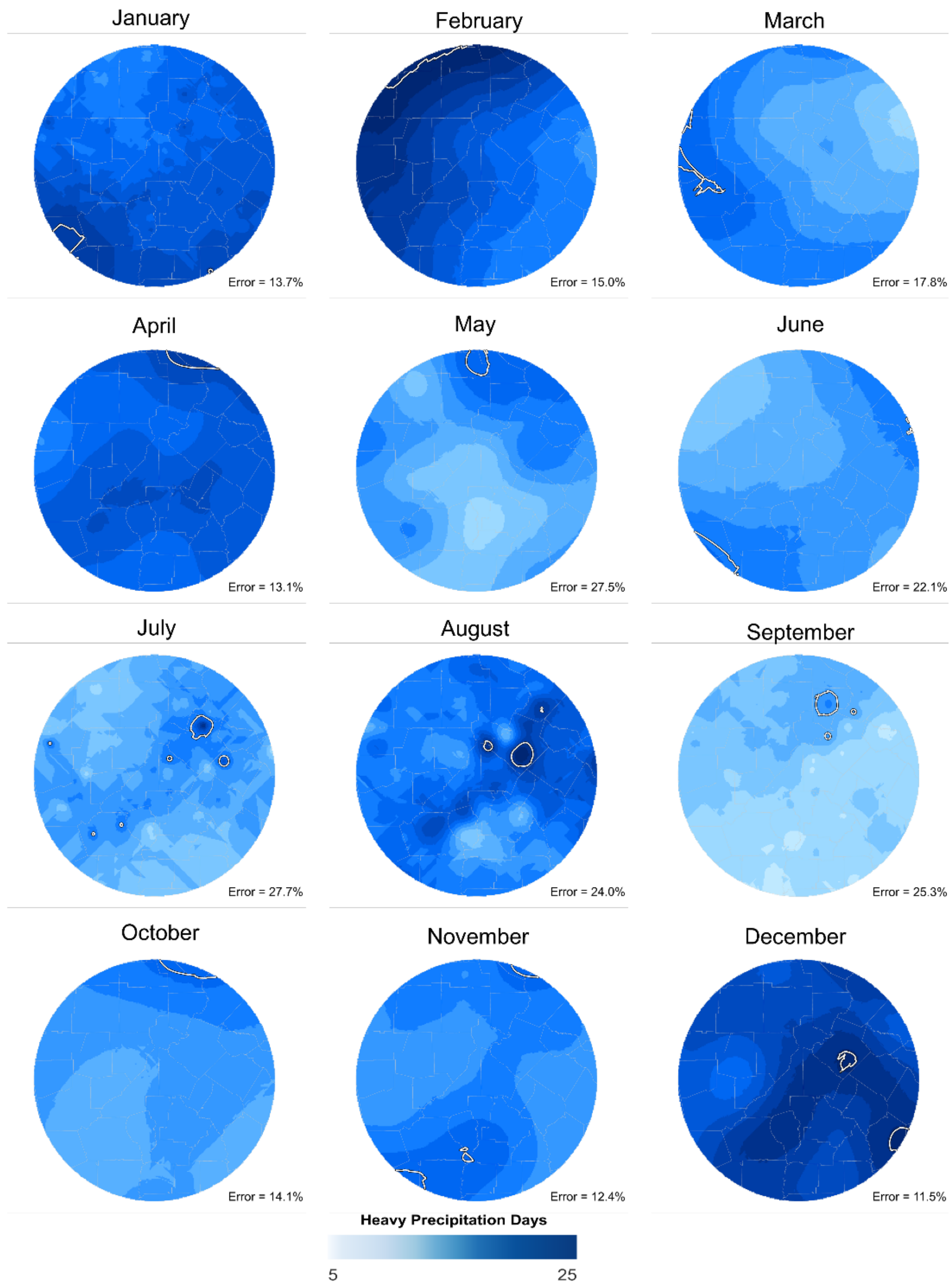

Figure 5.8 Month-specific surfaces of cumulative frequencies of heavy-precipitation days for the Atlanta region over 2014-2013 with the cross-validated percent error on each surface. White contour lines outline areas with the top 1% of values.

5.4 Month-specific correlations between mean imperviousness 20 to 80 km upwind of gauges

Significant positive correlations between upwind impervious surfaces and precipitation values occurred only during May and July-December (Figure 5.9). May exhibited significant correlations for PT at all distances except 20 to 40 km, a significant correlation for PD at all distances except 20 km, and only one significant correlation (at 80 km) for HPD. In July, significant correlations for PT and PD were observed from 20 km to 70 km, while no significant correlations were found for HPD. In August, significant correlations for PT were observed at all distances, there were no significant correlations for PD, and significant correlations for HPD occurred at all distances except 20 km. The only significant correlations in September occurred from 50 to 80 km for HPD. October showed significant correlations for all three variables at 70 and 80 km. November had significant correlations for PD from 30 km to 80 km, and December showed significant correlations for HPD at 20 km and 30 km.

Significant negative correlations between upwind impervious surfaces and precipitation values occurred only in February and March (Figure 5.9). February exhibited significant correlations for PT at all distances except 60 to 80 km, no significant correlation for PD, and significant correlations for HPD occurred at all distances. In March, significant correlations for PT and HPD occurred at all distances, while no significant correlations were found for PD.

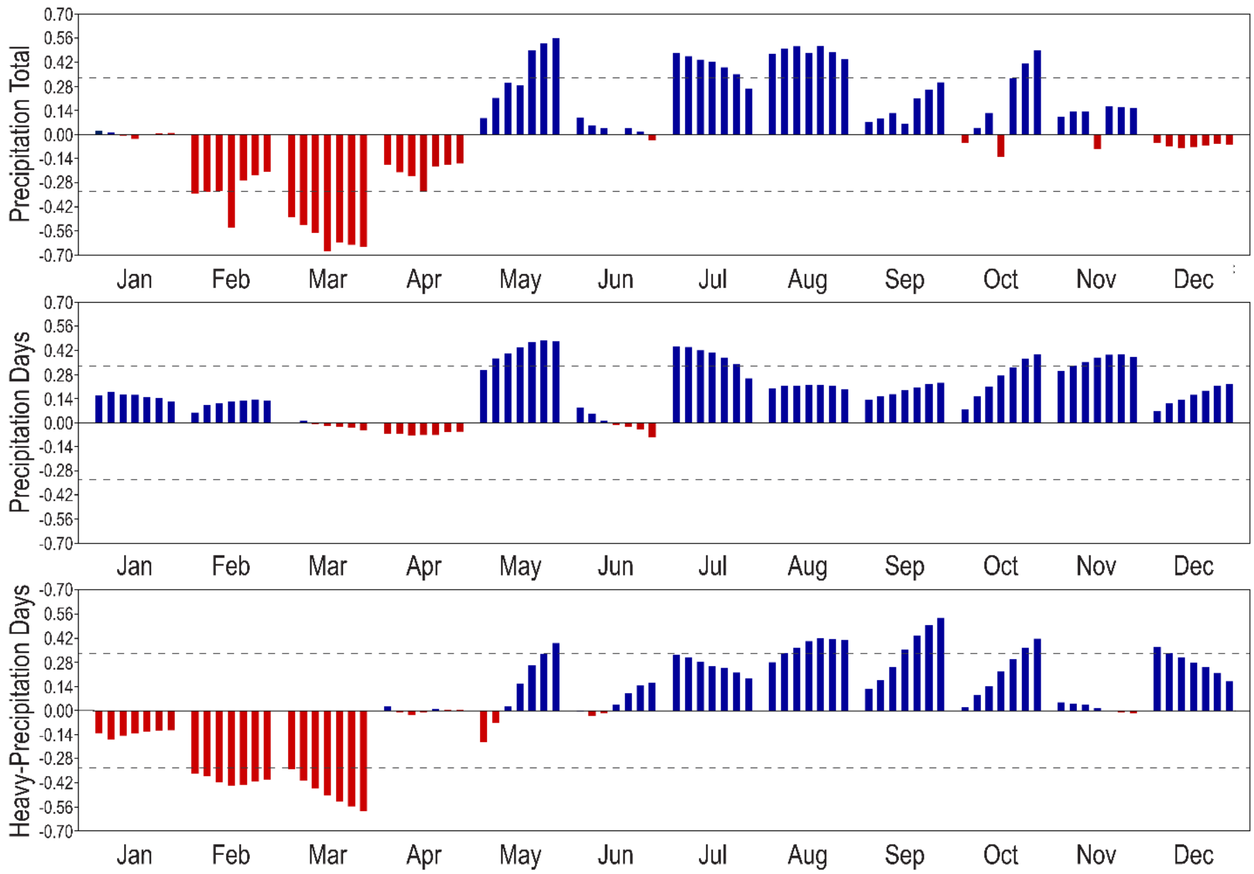

Figure 5.9 Month-specific correlations between mean imperviousness at distances ranging from 20 km to 80 km upwind of precipitation gauges and total precipitation, precipitation days, and heavy-precipitation days. For each month, the first bar is the correlation with 20-km upwind imperviousness and the last bar is the correlations with 80-km upwind imperviousness. Bars extending to or beyond the dashed lines are significant (α = 0.01, one-tailed).

5.5 Month-specific correlations between upwind imperviousness (20 to 80 km) and precipitation residuals

Significant positive correlations between upwind imperviousness and precipitation residuals were observed only during May, July, August, and December (Figure 5.10). In May, significant correlations for PT were found at distances of 60 to 80 km, except for 20 to 40 km, with a significant correlation for PD at 60 km and no statistically significant correlation for HPD. In July, significant correlations for PT and PD were observed across distances from 20 km to 70 km, but no significant correlations were found for HPD. In August, significant correlations for PT were present at all distances, while significant correlations for HPD were observed at all distances except for 20 km and 30 km, no significant correlations were found for PD. In September, the only significant correlation occurred at 80 km for HPD. Finally, in December, significant correlations for HPD were found at all distances except for 80 km, with no significant correlations for PT or PD.

Significant negative correlations between upwind imperviousness and precipitation residuals occurred only during February- April (Figure 5.10). In February and March, significant correlations for PT and HPD were found at all distances, while no significant correlations were found for PD. In April, significant correlations for PT occurred at all distances except 20km while there is no significant correlation for PD and HPD.

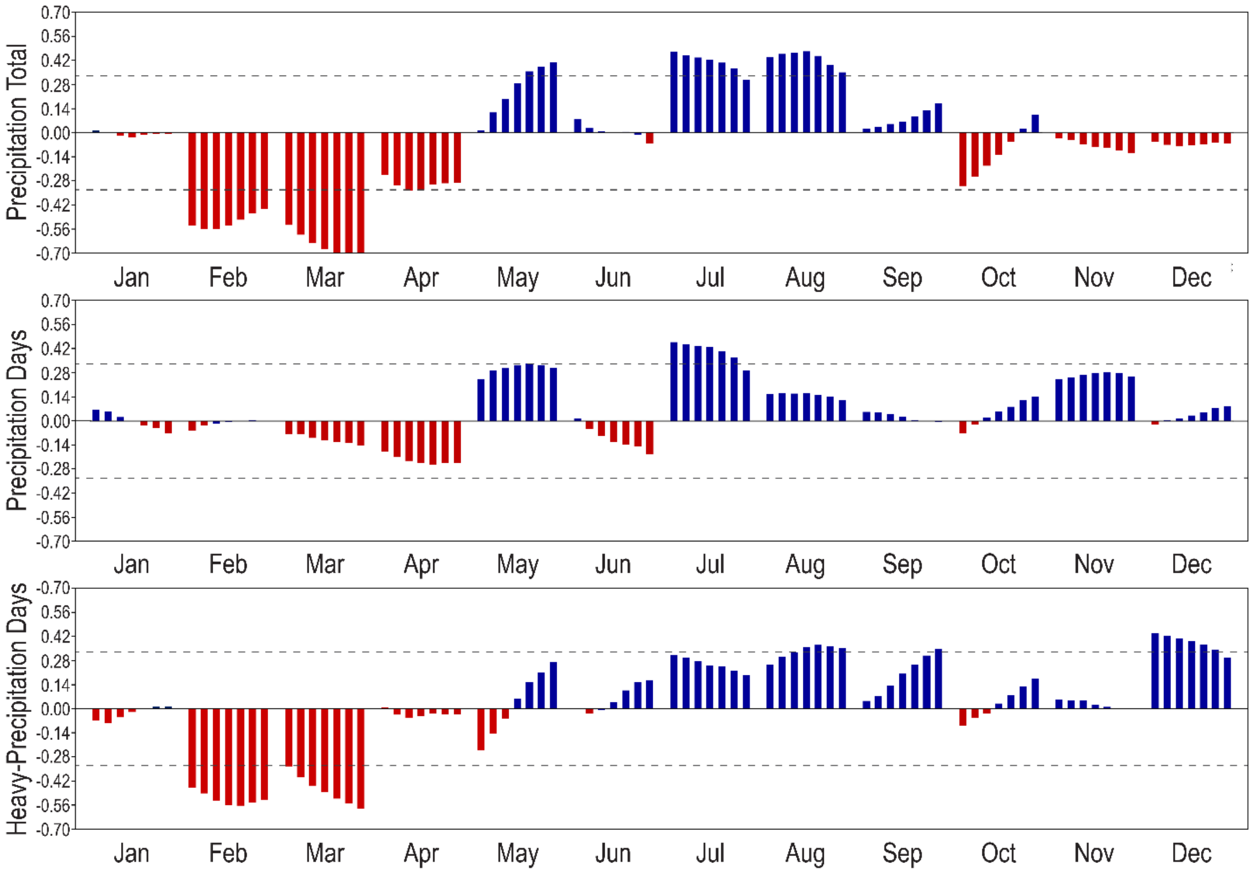

Figure 5.10 Month-specific correlations between upwind imperviousness (20 to 80 km) and precipitation and residuals of total precipitation, precipitation days, and heavy-precipitation days. The residuals were created by regressing each of the precipitation variables on elevation. For each month, the first bar is the correlation with 20-km upwind imperviousness and the last bar is the correlations with 80-km upwind imperviousness. Bars extending to or beyond the dashed lines are significant ($\alpha = 0.01$, one-tailed).

5.6 Downwind Precipitation vs Upwind Precipitation

Compared to upwind (control) gauges, downwind gauges tended to show lower precipitation totals during winter and early spring, while totals were higher in late spring and summer. Notably, precipitation totals at downwind gauges were significantly lower in March, with a reduction of approximately 10%. Conversely, downwind gauges recorded significantly higher totals in May, July, and August, with increases of around 20%.

Downwind gauges generally had more precipitation days compared to control gauges across most months. Significant differences were observed in May, July, August, and October, where downwind gauges saw more precipitation days. In May and July, downwind gauges experienced nearly 15% more precipitation days, while August and October saw increases of less than 10%.

Similar to precipitation totals, downwind gauges tended to have fewer heavy-precipitation days than control gauges in late winter and early spring and more heavy-precipitation days compared to control gauges from late spring to late summer. The only instance of significantly fewer heavy-precipitation days at downwind gauges compared to control gauges occurred in March. In contrast, significantly more heavy-precipitation days at downwind gauges compared to control gauges were recorded in May and September, with percentage increases ranging from 36% to 53%, the highest being in May.

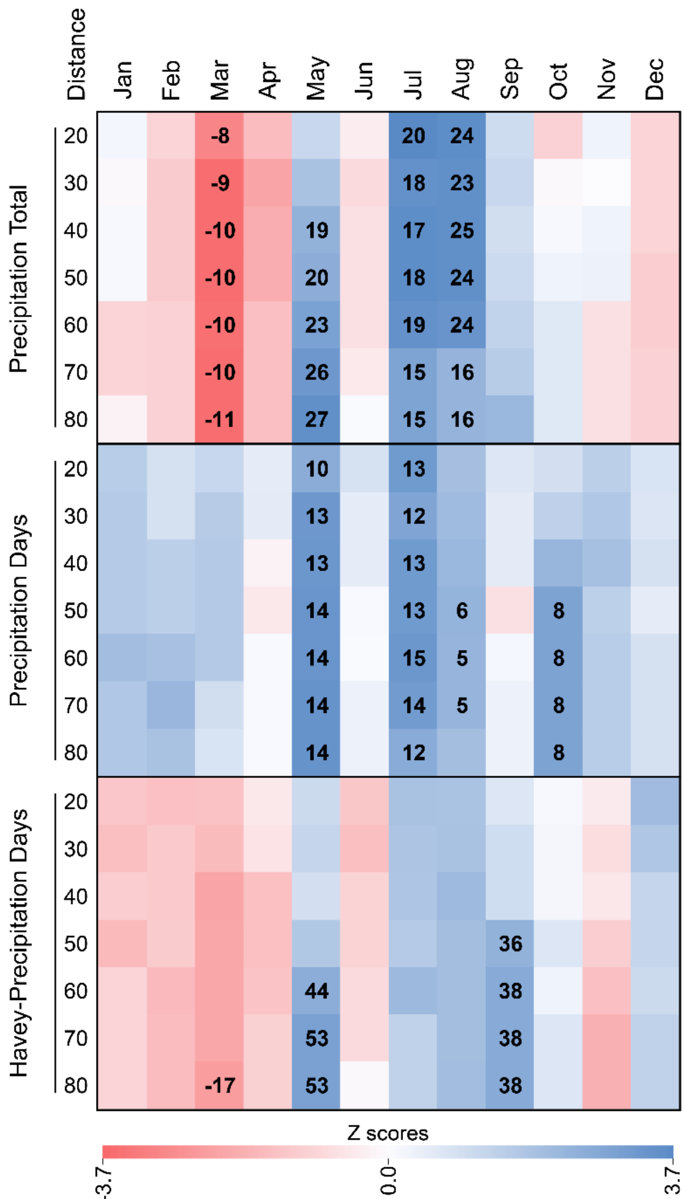

Figure 5.11 Heat map showing differences between downwind (urban-influenced) and control gauges within 60 km of downtown Atlanta. The figure is divided into precipitation totals, precipitation days, and heavy-precipitation days. Imperviousness-upwind distances range from 20 km to 80 km. The colors are Z score from Mann-Whitney U tests, with red (blue) indicating smaller (larger) precipitation values for downwind gauges compared to control gauges. Numeric values denote the percent difference (i.e., downwind vs. control) when the differences are statistically significant (α = 0.01 and one-tailed).

6 DISCUSSION

6.1 Precipitation Enhancement in Late Spring and Summer

The enhancement of precipitation totals and heavy-precipitation days in the Atlanta metropolitan area, which occurs mostly in DeKalb and Gwinnett counties (northeast and east of Atlanta), tends to occur predominantly during the late spring and summer months (Figures 5.6-5.8) These months coincide with higher values of Convective Available Potential Energy (CAPE), which is essential for the development of convective storms that produce significant rainfall (Lacke et al., 2009). The enhancement north/northeast of Atlanta during the warm seasons is consistent with several studies that have shown significant precipitation and lightning enhancement downwind of Atlanta (Bentley et al., 2012; Mote et al., 2007; Diem, 2008; McLeod et al., 2017; Diem and Mote, 2005; Shem and Shepherd, 2008; Rose et al., 2008; Stallins and Bentley, 2006; Burke and Shepherd, 2023; Stallins et al., 2006). This study found precipitation totals enhanced by 16% to 27% and heavy-precipitation days enhanced by 36% to 53% during May, July, and August, demonstrating stronger localized impacts in specific months of the warm season. These findings align with previous research, which has shown that a 20% increase in heavy precipitation days was found downwind of Atlanta for June-August (Diem, 2008) and 10% for May–September (Dixon and Mote, 2003); a 30% increase in daily average precipitation in June to August (Mote et al., 2007); and a flash density enhancement of 8.0 flashes km^{-2} yr^{-1} was observed in Gwinnett County, northeast of Atlanta (Stallins et al., 2006).

6.2 Precipitation Suppression in Late Winter and Early Spring

In contrast to the enhancement observed during the summer, suppression of precipitation totals and heavy-precipitation days occurs in February and March mostly in DeKalb and Gwinnett counties (Figures 5.6, 5.8-5.11). There was a significantly negative correlation in February and March for PT and HPD with March being the most significant (Figures 5.9-5.11). Precipitation totals and heavy-precipitation days are suppressed by 8% to 17 % in March (Figure 5.11). These results suggest that urban particulates likely reduce precipitation during late winter and early spring, especially when convective forces are less intense. Particulates can suppress precipitation by increasing cloud condensation nuclei (CCN) that slow droplet formation, which leads to reduced rainfall (Rosenfeld, 2000; Givati and Rosenfeld, 2004). Another study (Diem, 2013) shows HPD suppression in the Atlanta region during the summer months prior to the passage of the Clean Air Act. Only one other study has found contemporary rainfall suppression in urban areas (Barman and Gokhale, 2022), observing that black carbon aerosols reduce rainfall during the pre-monsoon period in northeast India by increasing atmospheric stability through the semi-direct effect, which suppresses cloud formation and convection, particularly in regions with higher terrain during cooler months when convection is weaker.

6.3 Aerosol Effects on Precipitation Days

Unlike precipitation totals and heavy-precipitation days, urbanization appears to increase precipitation days during most months (Figures 5.7, 5.9-5.11). Significant enhancement occurs during May, July, August, and October (Figures 5.7 and 5.11), and significant correlations occurred in May, June, October, and November (Figures 5.9 and 5.10). No recent contemporary study has specifically focused on the “precipitation days” variable in Atlanta; however, one study

(Dixon and Mote, 2003) has found an increase in precipitation days. An increase in precipitation days due to the urban heat island effect occurred predominantly during the summer months, with a peak in July, while no UHI-initiated precipitation events were recorded in September (Dixon and Mote, 2003). Aerosol effects on clouds are the most likely explanation of increased precipitation days during the non-summer months, because aerosols usually increase cloud droplet numbers while reducing individual droplet sizes, slowing the coalescence process, and often prolonging cloud cover without intensifying rainfall (Tao et al., 2012). Urban aerosols can increase the frequency of light precipitation days by extending cloud duration rather than directly increasing rainfall intensity, as was found in certain regions in China, particularly in the summer months (Sun and Zhao, 2021). High aerosol levels also have been linked to delayed precipitation onset and a tendency for prolonged, lighter rainfall events rather than increased intensity (Givati and Rosenfeld, 2004; Han et al., 2011).

7 CONCLUSION

Through the analysis of precipitation patterns in the Atlanta region, this study has shown that urbanization has a significant effect on precipitation during most months. Precipitation totals and heavy-precipitation days were enhanced northeast and east of Atlanta (mostly in DeKalb and Gwinnett counties) in May, July, and August, while significant correlations were observed between upwind imperviousness and PT and HPD from May to October, with enhancements reaching up to 20% downwind for PT and 50% for HPD. Urbanization appears to increase precipitation days during most months, with significant enhancement downwind of Atlanta (north and northeast) occurring in May, July, August, and October, and significant correlations with imperviousness observed in May, June, October, and November, enhancing precipitation by about 5-15% downwind. Urbanization appears to suppress precipitation during late winter and early spring. The urban heat island effect is likely the dominant mechanisms responsible for the precipitation enhancement. The impact of urban aerosols on clouds is the likely cause of the suppression of precipitation totals and heavy-precipitation days and the increase in precipitation days. To improve the continuity of results and reduce the impact of outliers, future studies might consider using three-month overlapping periods rather than individual months.

REFERENCES

- Ali, H., Fowler, H. J., Lenderink, G., Lewis, E., & Pritchard, D. (2021). Consistent Large-Scale Response of Hourly Extreme Precipitation to Temperature Variation Over Land. Geophysical Research Letters, 48(4). ***https://doi.org/10.1029/2020gl090317***

- Arnfield, A. J. (2003). Two decades of urban climate research: a review of turbulence, exchanges of energy and water, and the urban heat island. *International Journal of Climatology*, *23*(1), 1–26. https://doi.org/10.1002/joc.859

- Ashley, W. S., Bentley, M. L., & Stallins, J. A. (2012). Urban-induced thunderstorm modification in the Southeast United States. *Climatic Change*, *113*(2), 481–498. https://doi.org/10.1007/s10584-011-0324-1

- Bentley, M. L., Stallins, J. A., & Ashley, W. S. (2012). Synoptic environments favourable for urban convection in Atlanta, Georgia. *International Journal of Climatology, 32*(8), 1287–1294. https://doi.org/10.1002/joc.2344

- Bornstein, R. D. (1968). Observations of the Urban Heat Island Effect in New York City. Journal of Applied Meteorology and Climatology, 7(4), 575-582. https://doi.org/10.1175/1520-0450(1968)007<0575:OOTUHI>2.0.CO;2

- Bornstein, R., & Lin, Q. (2000). Urban heat islands and summertime convective thunderstorms in Atlanta: three case studies. *Atmospheric Environment*, *34*(3), 507–516. https://doi.org/10.1016/s1352-2310(99)00374-x

- Chang, C., Li, Y., Chen, Y., Huang, J. J., & Zhang, Y. (2021). Advanced statistical analyses of urbanization impacts on heavy rainfall in the Beijing metropolitan area. *Urban Climate*, *40*, 100987. https://doi.org/10.1016/j.uclim.2021.100987

- Cicek, I., & Turkoglu, N. (2005). Urban effects on precipitation in Ankara. Atmósfera, 18(3), 173-187.
- Daly, C., Halbleib, M., Smith, J. I., Gibson, W. P., Doggett, M. K., Taylor, G. H., Curtis, J., & Pasteris, P. P. (2008). Physiographically sensitive mapping of climatological temperature and precipitation across the conterminous United States. International Journal of Climatology, 28(15), 2031–2064. https://doi.org/10.1002/joc.1688
- Daly, C., Neilson, R. P., & Phillips, D. L. (1994). A Statistical-Topographic Model for Mapping Climatological Precipitation over Mountainous Terrain. Journal of Applied Meteorology and Climatology, 33(2), 140-158. https://doi.org/10.1175/1520-0450(1994)033<0140:ASTMFM>2.0.CO;2
- Daniels, E. E., Lenderink, G., Hutjes, R. W. A., & Holtslag, A. A. M. (2015). Observed urban effects on precipitation along the Dutch West coast. *International Journal of Climatology*, *36*(4), 2111–2119. https://doi.org/10.1002/joc.4458
- Debbage, N., & Shepherd, J. M. (2015). The urban heat island effect and city contiguity. *Computers, Environment and Urban Systems*, *54*, 181–194. https://doi.org/10.1016/j.compenvurbsys.2015.08.002
- Deng, Z., Wang, Z., Wu, X., Lai, C., & Liu, W. (2023). Effect difference of climate change and urbanization on extreme precipitation over the Guangdong-Hong Kong-Macao Greater Bay Area. *Atmospheric Research*, *282*, 106514. https://doi.org/10.1016/j.atmosres.2022.106514
- Deng, Z., Wang, Z., Wu, X., Lai, C., & Liu, W. (2023). Effect difference of climate change and urbanization on extreme precipitation over the Guangdong-Hong Kong-Macao Greater

Bay Area. *Atmospheric Research*, *282*, 106514. https://doi.org/10.1016/j.atmosres.2022.106514

- Diem, J. E. (2008). Detecting summer rainfall enhancement within metropolitan Atlanta, Georgia USA. *International Journal of Climatology*, *28*(1), 129–133. https://doi.org/10.1002/joc.1560
- Diem, J. E. (2012). Influences of the Bermuda High and atmospheric moistening on changes in summer rainfall in the Atlanta, Georgia region, USA. International Journal of Climatology, 33(1), 160–172. https://doi.org/10.1002/joc.3421
- Diem, J. E. (2013). The 1970 Clean Air Act and termination of rainfall suppression in a U.S. urban area. Atmospheric Environment, 75, 141–146. https://doi.org/10.1016/j.atmosenv.2013.04.041
- Diem, J. E., & Brown, D. P. (2003). Anthropogenic Impacts on Summer Precipitation in Central Arizona, U.S.A. *The Professional Geographer*, *55*(3), 343–355. https://doi.org/10.1111/0033-0124.5503011
- Diem, J. E., Coleman, L. B., Digirolamo, P. A., Gowens, C. W., Hayden, N. R., Unger, E. E., Wetta, G. B., & Williams, H. A. (2004). Comments on “Rainfall Modification by Major Urban Areas: Observations from Spaceborne Rain Radar on the TRMM Satellite”. Journal of Applied Meteorology, 43(6), 941-950. https://doi.org/10.1175/1520-0450(2004)043<0941:CORMBM>2.0.CO;2
- Diem, J. E., & Mote, T. L. (2005). Interepochal Changes in Summer Precipitation in the Southeastern United States: Evidence of Possible Urban Effects near Atlanta, Georgia. *Journal of Applied Meteorology*, *44*(5), 717–730. https://doi.org/10.1175/jam2221.1

- Dixon, P. G., & Mote, T. L. (2003). Patterns and Causes of Atlanta's Urban Heat Island–Initiated Precipitation. Journal of Applied Meteorology, 42(9), 1273-1284. https://doi.org/10.1175/1520-0450(2003)042<1273:PACOAU>2.0.CO;2
- Draxler, R. R. (1986). Simulated and Observed Influence of the Nocturnal Urban Heat Island on the Local Wind Field. Journal of Applied Meteorology and Climatology, 25(8), 1125-1133. https://doi.org/10.1175/1520-0450(1986)025<1125:SAOIOT>2.0.CO;2
- Estoque, R. C., Murayama, Y., & Myint, S. W. (2017). Effects of landscape composition and pattern on land surface temperature: An urban heat island study in the megacities of Southeast Asia. *Science of the Total Environment*, *577*, 349–359. https://doi.org/10.1016/j.scitotenv.2016.10.195
- Fagnant, C., Gori, A., Sebastian, A., Bedient, P. B., & Ensor, K. B. (2020). Characterizing spatiotemporal trends in extreme precipitation in Southeast Texas. *Natural Hazards*, *104*(2), 1597–1621. https://doi.org/10.1007/s11069-020-04235-x
- Feng, H., Zou, B., & Tang, Y. (2017). Scale- and Region-Dependence in Landscape-PM2.5 Correlation: Implications for Urban Planning. *Remote Sensing*, *9*(9), 918. https://doi.org/10.3390/rs9090918
- Georgescu, M., Moustaoui, M., Mahalov, A., & Dudhia, J. (2012). Summer-time climate impacts of projected megapolitan expansion in Arizona. *Nature Climate Change*, *3*(1), 37–41. https://doi.org/10.1038/nclimate1656
- GUHATHAKURTA, P., SREEJITH, O. P., & MENON, P. A. (2011). Impact of climate change on extreme rainfall events and flood risk in India. *Journal of Earth System Science*, *120*(3), 359–373. https://doi.org/10.1007/s12040-011-0082-5

- Gunawardena, K., Wells, M., & Kershaw, T. (2017). Utilising green and bluespace to mitigate urban heat island intensity. *Science of the Total Environment*, *584–585*, 1040–1055. https://doi.org/10.1016/j.scitotenv.2017.01.158
- Güneralp, B., Reba, M., Hales, B. U., Wentz, E. A., & Seto, K. C. (2020). Trends in urban land expansion, density, and land transitions from 1970 to 2010: a global synthesis. *Environmental Research Letters*, *15*(4), 044015. https://doi.org/10.1088/1748-9326/ab6669
- Haberlie, A. M., Ashley, W. S., & Pingel, T. J. (2014). The effect of urbanisation on the climatology of thunderstorm initiation. Quarterly Journal of the Royal Meteorological Society, 141(688), 663–675. https://doi.org/10.1002/qj.2499
- Han, J., Baik, J., & Khain, A. P. (2011). A Numerical Study of Urban Aerosol Impacts on Clouds and Precipitation. Journal of the Atmospheric Sciences, 69(2), 504–520. https://doi.org/10.1175/jas-d-11-071.1
- Hou, H., Su, H., Yao, C., & Wang, Z. H. (2023). Spatiotemporal patterns of the impact of surface roughness and morphology on urban heat island. *Sustainable Cities and Society*, *92*, 104513. https://doi.org/10.1016/j.scs.2023.104513
- Huang, X., Liu, Z., Ge, Y., Li, Q., Wang, X., Fu, H., Zhu, J., Zhou, B., Wang, L., George, C., Wang, Y., Wang, X., Su, J., Xue, L., Yu, S., Mellouki, A., & Chen, J. (2023). Aerosol high water contents favor sulfate and secondary organic aerosol formation from fossil fuel combustion emissions. *Npj Climate and Atmospheric Science*, *6*(1). https://doi.org/10.1038/s41612-023-00504-1

- Huff, F. A. , & Changnon , S. A. , Jr. (1972). Climatological Assessment of Urban Effects on Precipitation at St. Louis. Journal of Applied Meteorology and Climatology, 11(5), 823-842. https://doi.org/10.1175/1520-0450(1972)011<0823:CAOUEO>2.0.CO;2
- Islam, S., Villarini, G., & Zhang, W. (2023). Quantification of the role of urbanization in changing the rainfall associated with tropical cyclones affecting Charlotte, North Carolina. *Urban Climate*, *52*, 101681. https://doi.org/10.1016/j.uclim.2023.101681
- Jauregui, E., & Romales, E. (1996). Urban effects on convective precipitation in Mexico city. *Atmospheric Environment*, *30*(20), 3383–3389. https://doi.org/10.1016/1352-2310(96)00041-6
- Jin, M., Shepherd, J. M., & King, M. D. (2005). Urban aerosols and their variations with clouds and rainfall: A case study for New York and Houston. Journal of Geophysical Research Atmospheres, 110(D10). https://doi.org/10.1029/2004jd005081
- Jo, E., Park, C., Son, S. W., Roh, J. W., Lee, G. W., & Lee, Y. H. (2020). Classification of Localized Heavy Rainfall Events in South Korea. *Asia-Pacific Journal of Atmospheric Sciences*, *56*(1), 77–88. https://doi.org/10.1007/s13143-019-00128-7
- Kondratyeva, A., Knapp, S., Durka, W., Kühn, I., Vallet, J., Machon, N., Martin, G., Motard, E., Grandcolas, P., & Pavoine, S. (2020). Urbanization Effects on Biodiversity Revealed by a Two-Scale Analysis of Species Functional Uniqueness vs. Redundancy. *Frontiers in Ecology and Evolution*, *8*. https://doi.org/10.3389/fevo.2020.00073
- Kundell, J. E. & Myszewski, M. (2002). Urban Sprawl. In New Georgia Encyclopedia. Retrieved Jun 8, 2017, from https://www.georgiaencyclopedia.org/articles/arts-culture/urban-sprawl/

- Lacke, M. C., Mote, T. L., & Shepherd, J. M. (2009). Aerosols and associated precipitation patterns in Atlanta. Atmospheric Environment, 43(28), 4359–4373. https://doi.org/10.1016/j.atmosenv.2009.04.022
- Le, L. T., Tang-Huang, L., Le, C. V., Pham, L. T., Le, H. T. T., Nguyen, L. Q., Nguyen, N. V., & Cao, C. X. (2019). Retrieval of Aerosol Optical Depth Using Satellite Data Associated with Ground-based Observations over Urban and Rural Areas. *Kartografija I Geoinformacije*, *18*(32), 4–17. https://doi.org/10.32909/kg.18.32.1
- Li, G., Fang, C., Li, Y., Wang, Z., Sun, S., He, S., Qi, W., Bao, C., Ma, H., Fan, Y., Feng, Y., & Liu, X. (2022). Global impacts of future urban expansion on terrestrial vertebrate diversity. *Nature Communications*, *13*(1). https://doi.org/10.1038/s41467-022-29324-2
- Liang, L., & Gong, P. (2020). Urban and air pollution: a multi-city study of long-term effects of urban landscape patterns on air quality trends. *Scientific Reports*, *10*(1). https://doi.org/10.1038/s41598-020-74524-9
- Liu, J., & Niyogi, D. (2019). Meta-analysis of urbanization impact on rainfall modification. *Scientific Reports*, *9*(1). https://doi.org/10.1038/s41598-019-42494-2
- Liu, J., Schlünzen, K. H., Frisius, T., & Tian, Z. (2021). Effects of urbanization on precipitation in Beijing. *Physics and Chemistry of the Earth, Parts a/B/C*, *122*, 103005. https://doi.org/10.1016/j.pce.2021.103005
- Liu, Z., He, C., & Wu, J. (2016). The Relationship between Habitat Loss and Fragmentation during Urbanization: An Empirical Evaluation from 16 World Cities. *PLOS ONE*, *11*(4), e0154613. https://doi.org/10.1371/journal.pone.0154613

- Lorenz, J. M., Kronenberg, R., Bernhofer, C., & Niyogi, D. (2019). Urban Rainfall Modification: Observational Climatology Over Berlin, Germany. *Journal of Geophysical Research: Atmospheres*, *124*(2), 731–746. https://doi.org/10.1029/2018jd028858
- Lu, M., Yu, Z., Hua, J., Kang, C., & Lin, Z. (2023). Spatial dependence of floods shaped by extreme rainfall under the influence of urbanization. *Science of the Total Environment*, *857*, 159134. https://doi.org/10.1016/j.scitotenv.2022.159134
- Luqman, M., Rayner, P. J., & Gurney, K. R. (2023). On the impact of urbanisation on CO2 emissions. *Npj Urban Sustainability*, *3*(1). https://doi.org/10.1038/s42949-023-00084-2
- McLeod, J., Shepherd, M., & Konrad, C. E. (2017). Spatio-temporal rainfall patterns around Atlanta, Georgia and possible relationships to urban land cover. *Urban Climate*, *21*, 27–42. https://doi.org/10.1016/j.uclim.2017.03.004
- Miao, S., Chen, F., Li, Q., & Fan, S. (2011). Impacts of Urban Processes and Urbanization on Summer Precipitation: A Case Study of Heavy Rainfall in Beijing on 1 August 2006. *Journal of Applied Meteorology and Climatology*, *50*(4), 806–825. https://doi.org/10.1175/2010jamc2513.1
- Mote, T. L., Lacke, M. C., & Shepherd, J. M. (2007). Radar signatures of the urban effect on precipitation distribution: A case study for Atlanta, Georgia. *Geophysical Research Letters*, *34*(20). https://doi.org/10.1029/2007gl031903
- Mou, Y., Gao, X., Yang, Z., Xu, T., & Feng, J. (2022). Variation characteristics and the impact of urbanization of extreme precipitation in Shanghai. *Scientific Reports*, *12*(1). https://doi.org/10.1038/s41598-022-22352-4

- Mukherjee, S., Aadhar, S., Stone, D., & Mishra, V. (2018). Increase in extreme precipitation events under anthropogenic warming in India. *Weather and Climate Extremes*, *20*, 45–53. https://doi.org/10.1016/j.wace.2018.03.005
- Oke, T. (1973). City size and the urban heat island. *Atmospheric Environment (1967)*, *7*(8), 769–779. https://doi.org/10.1016/0004-6981(73)90140-6
- Oke TR (1987). Boundary Layer Climates (2an Ed.), New York, Methuen and Co. Ltd
- Rajeswari, J. R., Srinivas, C. V., Yesubabu, V., Hari Prasad, D., & Venkatraman, B. (2021). Impacts of Urbanization, Aerodynamic Roughness, and Land Surface Processes on the Extreme Heavy Rainfall Over Chennai, India. *Journal of Geophysical Research: Atmospheres*, *126*(10). https://doi.org/10.1029/2020jd034017
- Rath, S. S., Panda, J., & Mohanty, S. (2021). Urban Transition and Its Impact on Mesoscale Weather. In Advances in geospatial technologies book series (pp. 187–216). https://doi.org/10.4018/978-1-7998-2249-3.ch007
- Rose, L. S., Stallins, J. A., & Bentley, M. L. (2008). Concurrent Cloud-to-Ground Lightning and Precipitation Enhancement in the Atlanta, Georgia (United States), Urban Region. Earth Interactions, 12(11), 1–30. https://doi.org/10.1175/2008ei265.1
- Rosenfeld, D. (2000). Suppression of Rain and Snow by Urban and Industrial Air Pollution. *Science*, *287*(5459), 1793–1796. https://doi.org/10.1126/science.287.5459.1793
- Shem, W., & Shepherd, M. (2008). On the impact of urbanization on summertime thunderstorms in Atlanta: Two numerical model case studies. Atmospheric Research, 92(2), 172–189. https://doi.org/10.1016/j.atmosres.2008.09.013

- Shepherd, J. M., Pierce, H., & Negri, A. J. (2002). Rainfall Modification by Major Urban Areas: Observations from Spaceborne Rain Radar on the TRMM Satellite. Journal of Applied Meteorology, 41(7), 689-701. https://doi.org/10.1175/1520-0450(2002)041<0689:RMBMUA>2.0.CO;2
- Simkin, R. D., Seto, K. C., McDonald, R. I., & Jetz, W. (2022). Biodiversity impacts and conservation implications of urban land expansion projected to 2050. *Proceedings of the National Academy of Sciences*, *119*(12). https://doi.org/10.1073/pnas.2117297119
- Singh, J., Karmakar, S., PaiMazumder, D., Ghosh, S., & Niyogi, D. (2020). Urbanization alters rainfall extremes over the contiguous United States. *Environmental Research Letters*, *15*(7), 074033. https://doi.org/10.1088/1748-9326/ab8980
- Stallins, J. A., & Bentley, M. L. (2006). Urban lightning climatology and GIS: An analytical framework from the case study of Atlanta, Georgia. Applied Geography, 26(3–4), 242–259.
- Stallins, J., Bentley, M., & Rose, L. (2006). Cloud-to-ground flash patterns for Atlanta, Georgia (USA) from 1992 to 2003. Climate Research, 30, 99–112. https://doi.org/10.3354/cr030099
- Steensen, B. M., Marelle, L., Hodnebrog, Ø., & Myhre, G. (2022). Future urban heat island influence on precipitation. Climate Dynamics, 58(11–12), 3393–3403. https://doi.org/10.1007/s00382-021-06105-z
- Sun, Y., & Zhao, C. (2021). Distinct impacts on precipitation by aerosol radiative effect over three different megacity regions of eastern China. Atmospheric Chemistry and Physics, 21(21), 16555–16574. https://doi.org/10.5194/acp-21-16555-2021

- Tao, W., Chen, J., Li, Z., Wang, C., & Zhang, C. (2012). Impact of aerosols on convective clouds and precipitation. Reviews of Geophysics, 50(2). https://doi.org/10.1029/2011rg000369

- Tao, W. K., Li, X., Khain, A., Matsui, T., Lang, S., & Simpson, J. (2012). The impact of aerosols on cloud and precipitation processes: cloud-resolving model simulations. *2012 IEEE International Geoscience and Remote Sensing Symposium*. https://doi.org/10.1109/igarss.2012.6351003

- *Urban Areas Facts*. (2021, October 8). Census.gov. https://www.census.gov/programs-surveys/geography/guidance/geo-areas/urban-rural/ua-facts.html

- Wang, H., Fu, R., Kumar, A., & Li, W. (2010). Intensification of Summer Rainfall Variability in the Southeastern United States during Recent Decades. *Journal of Hydrometeorology*, *11*(4), 1007–1018. https://doi.org/10.1175/2010jhm1229.1

- Wang, Z., Xie, Y., Mu, M., Feng, L., Xie, N., & Cui, N. (2022). Materials to Mitigate the Urban Heat Island Effect for Cool Pavement: A Brief Review. *Buildings*, *12*(8), 1221. https://doi.org/10.3390/buildings12081221

- Xiao, C., Wu, P., Zhang, L., & Song, L. (2016). Robust increase in extreme summer rainfall intensity during the past four decades observed in China. *Scientific Reports*, *6*(1). https://doi.org/10.1038/srep38506

- Yang, M., Wang, H., Yu, C. W., & Cao, S. J. (2022). A global challenge of accurately predicting building energy consumption under urban heat island effect. *Indoor and Built Environment*, *32*(3), 455–459. https://doi.org/10.1177/1420326x221123222

- Yilmaz, A. G., & Perera, B. J. C. (2015). Spatiotemporal Trend Analysis of Extreme Rainfall Events in Victoria, Australia. *Water Resources Management*, *29*(12), 4465–4480. https://doi.org/10.1007/s11269-015-1070-3
- Yu, X., Gu, X., Kong, D., Zhang, Q., Cao, Q., Slater, L. J., Ren, G., Luo, M., Li, J., Liu, J., Cheng, J., & Li, Y. (2022). Asymmetrical Shift Toward Less Light and More Heavy Precipitation in an Urban Agglomeration of East China: Intensification by Urbanization. *Geophysical Research Letters*, *49*(4). https://doi.org/10.1029/2021gl097046
- Zhang, W., Villarini, G., Vecchi, G. A., & Smith, J. A. (2018). *Urbanization exacerbated the rainfall and flooding caused by hurricane Harvey in Houston*. Nature. https://doi.org/10.1038/s41586-018-0676-z
- Zhang, X. Q. (2016). The trends, promises and challenges of urbanisation in the world. *Habitat International*, *54*, 241–252. https://doi.org/10.1016/j.habitatint.2015.11.018